Supporting Information

How fast can minibasins translate down a slope?

Observations from 2D numerical models

Naiara Fernandez[1]*, Oliver B. Duffy[1], Christopher A-L. Jackson[2,3], Boris J.P. Kaus[4], Tim Dooley[1], Michael Hudec[1]

[1]*Bureau of Economic Geology, Jackson School of Geosciences, The University of Texas at Austin, University Station, Box X, Austin, Texas, 78713-8924, USA*
[2]*Basins Research Group (BRG), Department of Earth Science & Engineering, Imperial College, Prince Consort Road, London, United Kingdom, SW7 2BP, UK*
[3]*Jacobs, 5 First Street, Manchester, M15 4GU, UK*
[4]*Institute of Geosciences, Johannes Gutenberg University Mainz J.-J.-Becher-Weg 21, D-55128 Mainz, Germany*

**Now at Helmholtz Centre Potsdam GFZ – German Research Centre for Geosciences*
Corresponding author: naiara@gfz-potsdam.de

Supporting Information

We provide the derivation of the analytical solution and supporting figures with definition of the equation terms. We also provide figures of additional numerical simulations that were performed with a salt thickness of 4 km.

Contents of this file

Derivation of Equations

A1. 1D channel flow

Here, we reproduce the steps as described in Turcotte and Schubert (2002) to derive the general expression for the velocity profile, *u(y)* of a viscous fluid in a channel that has the configuration shown in Fig. A1. Where τ indicates shear stress, and p, indicates pressure.

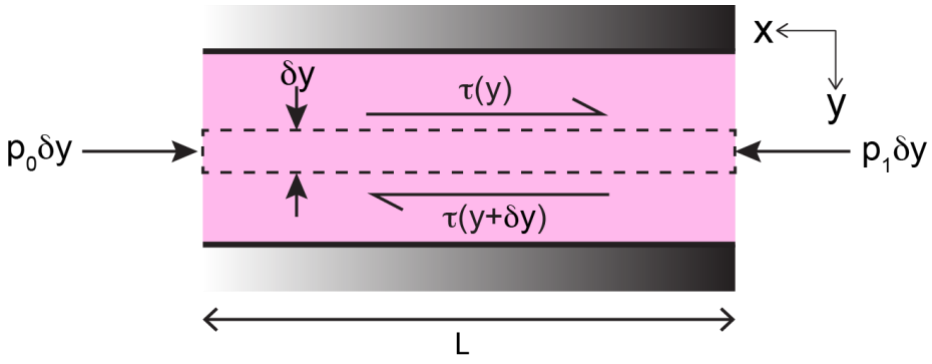

Figure SI-A1. Force balance in a channel with a viscous fluid (in pink) and pressure gradient in the x direction.

In the case of linear viscous fluids (with constant viscosity, μ), the shear stress, τ , at any location of the channel is given by:

$$\frac{du}{dy}\mu = \tau \qquad \text{(A1)}$$

The viscosity of the fluid, μ, is the constant of proportionality between the shear stress, τ, and the strain rate or velocity gradient, $\frac{du}{dy}$.

Flow in channel can be determined by the equation of motion, which implies a force balance on a layer of fluid of thickness δy and length L.

Net pressure force on the element in x direction is $(p_1 - p_0)\,\delta y$, which is the force per unit depth in the direction normal to the plane. For a 1-D channel flow, shear stress and velocity depend only on y.

Shear force on upper boundary of layer is $-\tau(y)L$ and at he lower boundary in x direction is:

$$\tau(y + \delta y)L = \left(\tau(y) + \frac{d\tau}{dy}\,\delta y\right) L \qquad \text{(A2)}$$

The net force in the layer is zero so we can rewrite as follows:

$$(p_1 - p_0)\delta y + \left(\tau(y) + \frac{d\tau}{dy}\,\delta y\right) L - \tau(y)L = 0 \qquad \text{(A3)}$$

$$\frac{d\tau}{dy} = -\frac{(p_1 - p_0)}{L} \qquad \text{(A4)}$$

$$\frac{dp}{dx} = -\frac{(p_1 - p_0)}{L} \qquad \text{(A5)}$$

$$\frac{d\tau}{dy} = \frac{dp}{dx} \qquad \text{(A6)}$$

By substituting $\frac{du}{dy}\mu = \tau$ in Eq. (A6), we obtain:

$$\mu\frac{d^2\tau}{dy^2} = \frac{dp}{dx} \qquad \text{(A7)}$$

Integration of the equation gives,

$$u = \frac{1}{\mu}\frac{dp}{dx}y^2 + C_1 y + C_2 \qquad \text{(A8)}$$

To evaluate the constants, we use the following boundary conditions, of u(h) = 0 and u(0) = u_0, which gives us the following general expression for the velocity in a 1D channel:

$$u = \frac{1}{2\mu}\frac{dp}{dx}(y^2 - hy) - \frac{u_0 y}{h} + u_0 \qquad \text{(A9)}$$

By substituting the Eq. (A9) into the Eq. (A1) of shear stress for viscous flows a general expression for the shear stress in a 1D channel is obtained:

$$\tau = \frac{1}{2}\frac{dp}{dx}(2y - h) - \frac{u_0 \mu}{h} \qquad \text{(A10)}$$

A2. 1D channel flow on an inclined plane

Now, instead of a horizontal channel, let's consider a constant thickness (h) layer of viscous fluid resting on an inclined plane as given in the Fig. A2.

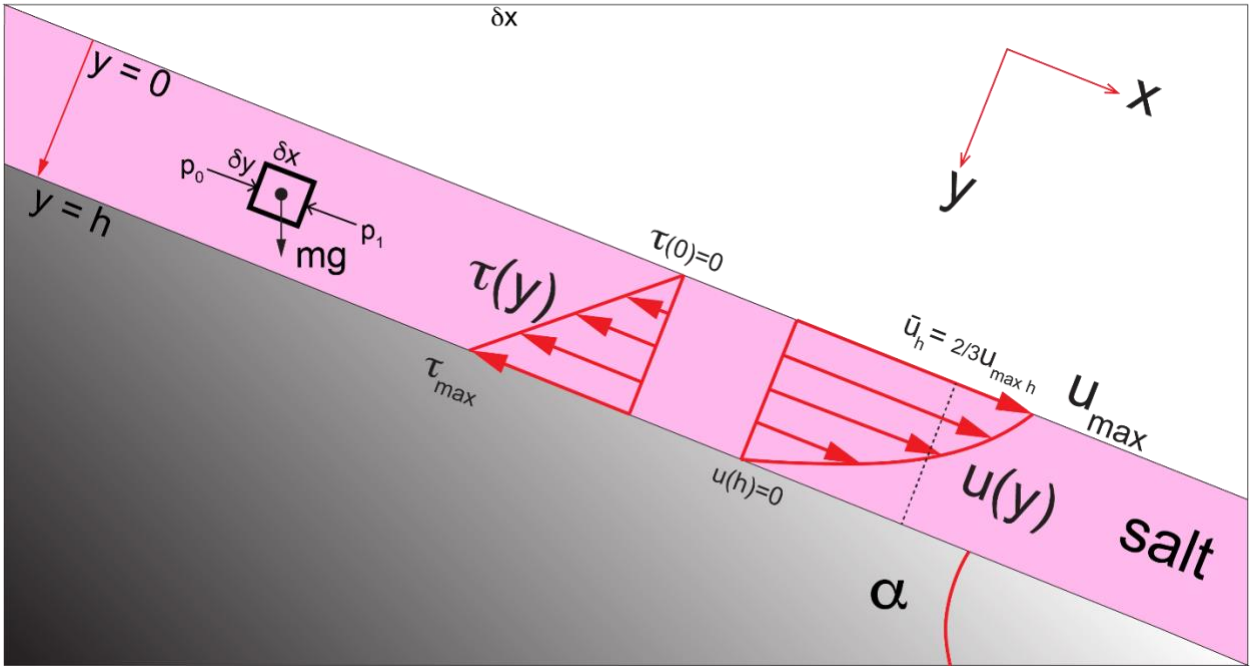

Figure SI-A2. Viscous fluid of constant thickness (in pink) resting on an inclined plane. The force balance in the channel is shown in a small element of dimensions $\delta x, \delta y$. Assuming a free-surface at the top and no-slip at the base of the viscous layer, the resulting velocity and shear stresses are shown.

We will again follow the steps given by Turcotte and Schubert (2002). First, we calculate the pressure gradient in the channel. If we consider a small unit element inside the channel with dimension of δx , δy and in equilibrium, the force in x is given by,

$$F_x = m\ g\ sin\alpha = \delta x\ \delta y\ \rho\ g\ sin\alpha \qquad \text{(A11)}$$

We can then calculate the pressure gradient along the x direction (parallel to the slope) as:

$$p_1 = p_0 + \frac{F_x}{\delta y} \qquad \text{(A12)}$$

$$\delta p = p_0 - p_1 = p_0 - \left(p_0 + \frac{\delta x\ \delta y\ \rho\ g\ sin\alpha}{\delta y}\right) = -\delta x\ \rho\ g\ sin\alpha \qquad \text{(A13)}$$

We can rearrange the equation as:

$$\frac{\delta p}{\delta x} = -\rho\ g\ sin\alpha \qquad \text{(A14)}$$

which is the pressure gradient in x direction due to the slope.

We can substitute the pressure gradient in the previously defined equation of motion in a channel due to pressure gradient (section A1) to obtain:

$$\frac{d\tau}{dy} = -\rho\ g\ sin\alpha \qquad \text{(A15)}$$

By integrating Eq. (A15), we can obtain $\tau(y)$ as:

$$\tau(y) = \int_0^y -\rho\ g\ sin\alpha\ \ dy = -\rho\ g\ sin\alpha\ y + C_1 \qquad \text{(A16)}$$

Assuming free-surface at y = 0, then $\tau(0) = 0$, then $C_1 = 0$.

Which gives a linear shear stress profile, increasing from 0 at the free surface to maximum shear stress at the no-slip base.

As given in Eq. (A1), for linear viscous fluids, we can relate the velocity gradient to the shear stress by the proportionality constant given by the viscosity, which is shown rewritten here:

$$\frac{du}{dy} = \frac{\tau}{\mu} \qquad \text{(A17)}$$

We can use Eq. (A16) and Eq. (17) to obtain the following:

$$u(y) = \int_0^y \frac{\tau}{\mu}\, dy = -\int_0^y \frac{\rho\, g\, sin\alpha\, y}{\mu}\, dy = -\frac{\rho\, g\, sin\alpha\, y^2}{\mu\, 2} + C_2 \qquad \text{(A18)}$$

Assuming no-slip boundary condition at base u(h) = 0, then $C_2 = \frac{\rho\, g\, sin\alpha\, h^2}{\mu\, 2}$. The velocity profile of a constant thickness viscous layer on an inclined plane is given by:

$$u(y) = -\frac{\rho\, g\, sin\alpha\, y^2}{\mu\, 2} + \frac{\rho\, g\, sin\alpha\, h^2}{\mu\, 2} = \frac{\rho\, g\, sin\alpha}{\mu\, 2}\,(h^2 - y^2) \qquad \text{(A19) or } \mathbf{Eq.\ (1)}$$

The velocity profile that results from a constant thickness layer with a free surface at the top, is not linear, but parabolic (as seen in the picture).

The maximum velocity at this case, occurs at the free-surface (y=0) where the shear stress is zero.

$$u_{\max\ h} = u(0) = \frac{\rho\, g\, sin\alpha\, h^2}{\mu\, 2} \qquad \text{(A20) or } \mathbf{Eq.\ (2)}$$

And the mean velocity can be obtained by integrating the velocity profile for the layer thickness and dividing it by the thickness.

$$u_{mean\,h} = \bar{u}_h = \frac{1}{h}\int_0^y u(y)\,dy = \frac{\rho\, g\, sin\alpha\, h^2}{\mu\, 3} = \frac{2}{3}u_{\max\, h} \qquad \text{(A21) or } \textbf{Eq. (3)}$$

Equations (1), (2) and (3) are the ones used in the main text.

A3. Velocity profiles for (sub-)layers defined within an inclined viscous layer

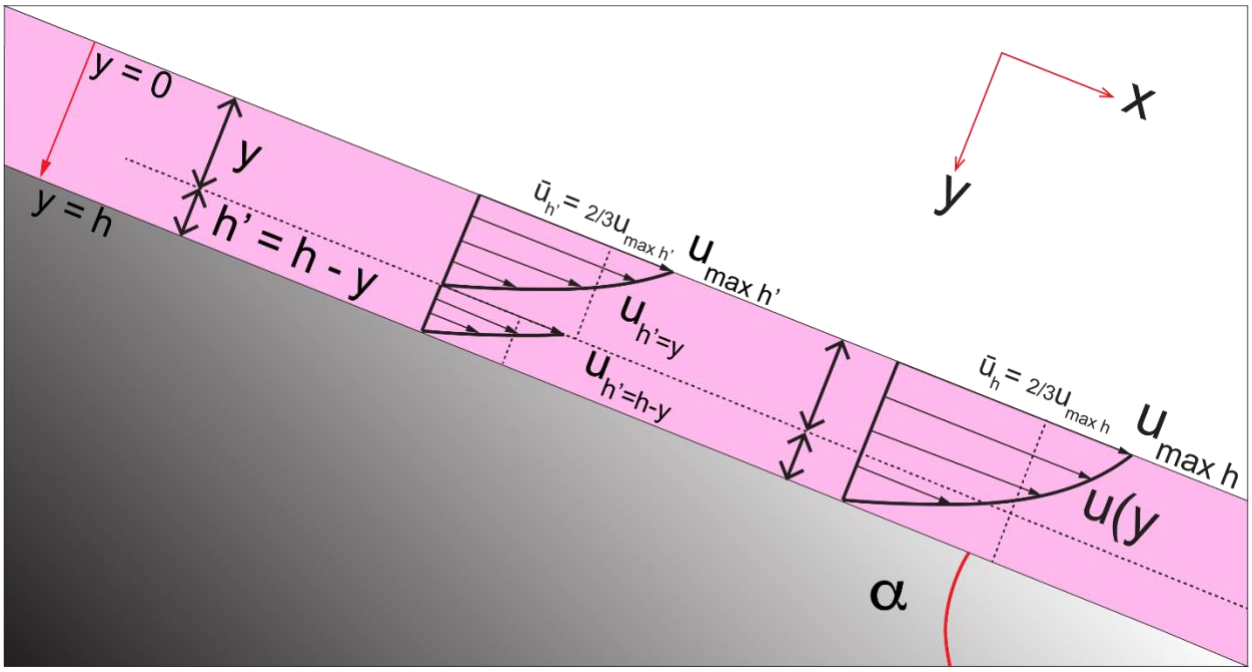

Figure SI-A3. Schematic illustration of the resulting velocity profiles when instead of the total thickness (h) of the viscous layer, partial thicknesses are considered. Upper portion where h'=y and lower portion where h'=h-y.

Now, instead of considering one unique velocity profile for the layer thickness of h of the entire viscous layer, we will consider the velocity profiles for (sub-)layers whose thicknesses, h', range between 0 and y (h'=y) and between y and h (h'=h-y) (see Fig. A3). In the case of h' = y, the maximum and mean velocities of the viscous (sub-)layers with thicknesses between 0 and y, can be calculated as:

$$u_{\max\, h'=y} = \frac{\rho\, g\, sin\alpha\, (y)^2}{\mu\, 2} \qquad \text{(A22)}$$

$$u_{\text{mean } h'} = \bar{u}_{h'=y} = \frac{\rho\, g\, sin\alpha\, (y)^2}{\mu\, 3} \qquad \text{(A23)}$$

Subtracting $u_{\max at\ y}$ from $u_{\max for\ h}$ gives the $u(y)$ of Eq. (A19) or Eq. (1):

$$u_{\max\ h} - u_{\max\ h'=y} = u(y) \qquad \text{(A24)}$$

Additionally, we consider the case of layers whose thicknesses h', range between y and h (h'=h-y). In this case, instead of having a unique value for the maximum and mean velocities, we have a range of values as given by:

$$u_{\max\ h'=h-y} = \frac{\rho\, g\, sin\alpha\, (h\prime)^2}{\mu\, 2} = \frac{\rho\, g\, sin\alpha\, (h-y)^2}{\mu\, 2} \qquad \text{(A25)}$$

$$\bar{u}_{h'=h-y} = \frac{\rho\, g\, sin\alpha\, (h')^2}{\mu\, 3} = \frac{\rho\, g\, sin\alpha\, (h-y)^2}{\mu\, 3} \qquad \text{(A26)}$$

A4. Minibasin on an inclined viscous layer

All the calculations in the previous sections consider the 1D flow channel equations. However, in the numerical models presented in the main text, minibasins are present in the slope. We will consider the minibasin being of the same density as the fluid, but a much higher viscosity (10^{25} Pa s). The viscosity of the minibasins is so high compared to the surrounding viscous fluid, that it effectively behaves as a rigid body, and it will translate down slope with a homogeneous velocity. These minibasins have a finite lateral extend, so there is a variation of velocity and shear stress along the x direction, which is not considered in the 1D channel flow equations. Despite this along X variation in velocity and shear stress, we can try to relate the minibasin velocity obtained from the models with the equations of 1D channel flows.

As in the previous section, we consider the viscous layer as divided in two portions from 0 to y and from y to h, but now we consider that y corresponds to the minibasin thickness, T_{mb}. See Fig. A4. The salt layer is then divided between 0 and y=T_{mb} and between y=T_{mb} and h. We will refer to these portions of the minibasin layer as upper portion and lower salt layer portion.

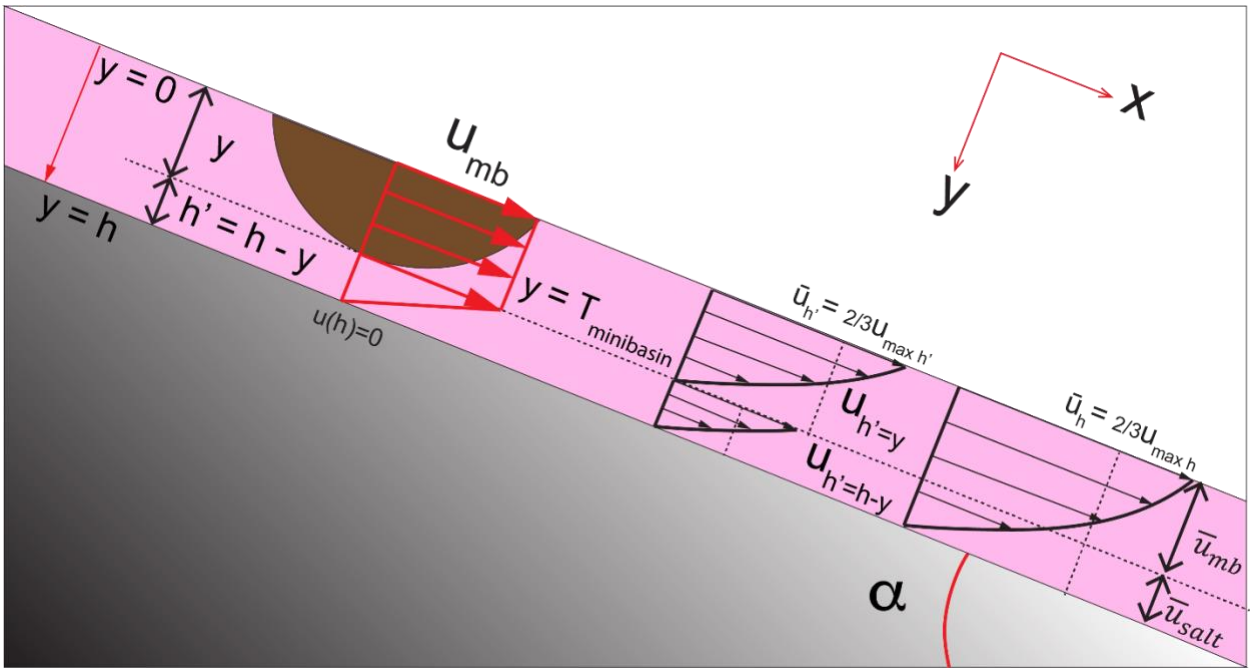

Figure SI-A4. Schematic illustration of the viscous layer (in pink) resting on an inclined plane. A minibasin (in brown) of density equal to that of the viscous fluid with a circular geometry is present in the viscous fluid. The thickness of the minibasin is T_{mb}.

The minibasins of the numerical simulations shown in this work, are sub-circular in shape, as illustrated in Fig. A4. However, we can also consider, rectangular shape minibasins with vertical walls and flat base as shown in Fig. A5.

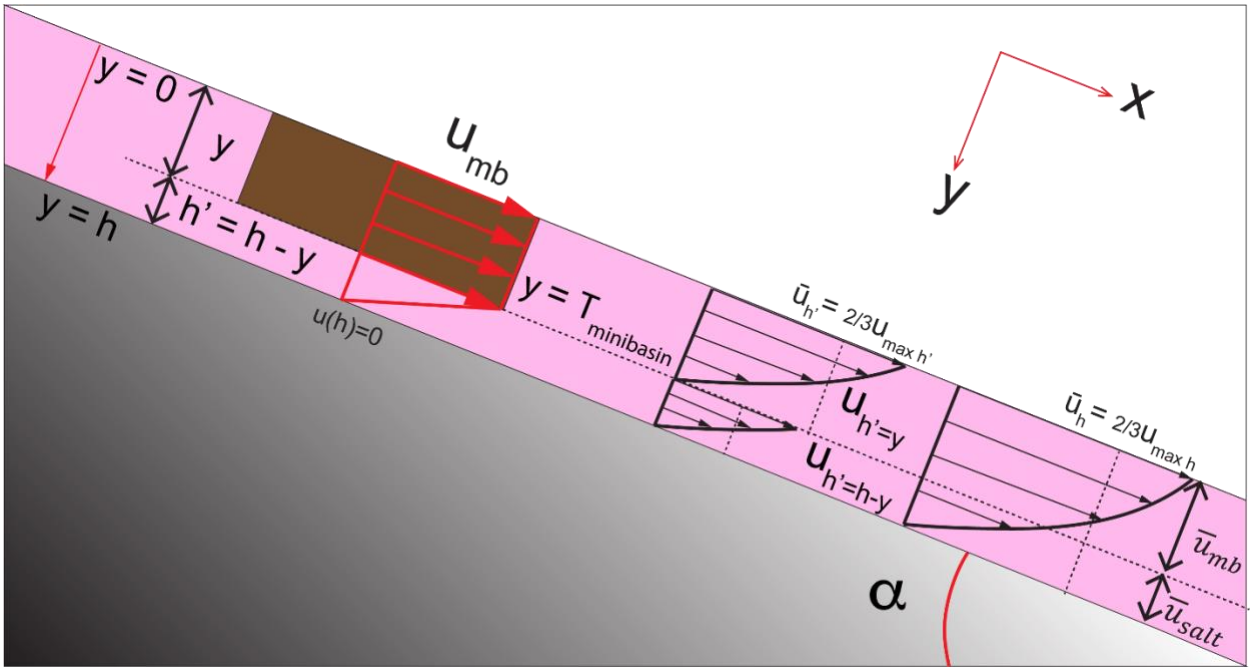

Figure SI-A5. Schematic illustration of the viscous layer (in pink) resting on an inclined plane. A minibasin (in brown) of density equal to that of the viscous fluid with a rectangular geometry is present in the viscous fluid. The thickness of the minibasin is T_{mb}.

Let's first consider the salt velocity profile calculated for the full thickness of the salt (h) and calculate the mean velocity of salt layer corresponding to the portions covering the minibasin thickness (upper portion) and the thickness below the minibasin (lower portion). We will call these velocities $\bar{u}_{mb}$ and $\bar{u}_{salt}$ respectively.

$$\bar{u}_{mb} = \frac{1}{y}\int_0^y u\,\partial y = \frac{1}{y}\frac{\rho\, g\, sin\alpha}{2\mu}\left(h^2 y - \frac{y^3}{3}\right) \qquad \text{(A27)}$$

$$\bar{u}_{salt} = \frac{1}{h-y}\int_{h-y}^{h} u\,\partial y = \frac{1}{h-y}\frac{\rho\, g\, sin\alpha}{2\mu}\left(\frac{2h^3}{3} - h^2 y - \frac{y^3}{3}\right) \qquad \text{(A28)}$$

Similarly, we can consider the equations from the previous section, where we calculated the maximum and mean velocity for viscous layers of thickness between 0 and h'=y, but now we consider y = T_{mb}.

$$u_{\max\ y=Tmb} = \frac{\rho\ g\ sin\alpha\ (y)^2}{\mu\ 2} \qquad \text{(A29)}$$

$$\bar{u}_{y=Tmb} = \frac{\rho\ g\ sin\alpha\ (y)^2}{\mu\ 3} \qquad \text{(A30)}$$

The equations for 1D channel flows are plotted in a normalized graph. The x-axis represents the velocities, normalized over the maximum velocity for a free-surface. T y-axis represents the thickness of a sub-portion of the total layer of thickness, normalized over the total thickness of the layer (h).

The results from the numerical simulations with minibasins can be plotted on the graph with the theoretical equations (minibasin velocity and thickness). Similarly, results of numerical models of rafts or sediment blocks (vertical walls, instead of circular walls) are plotted.

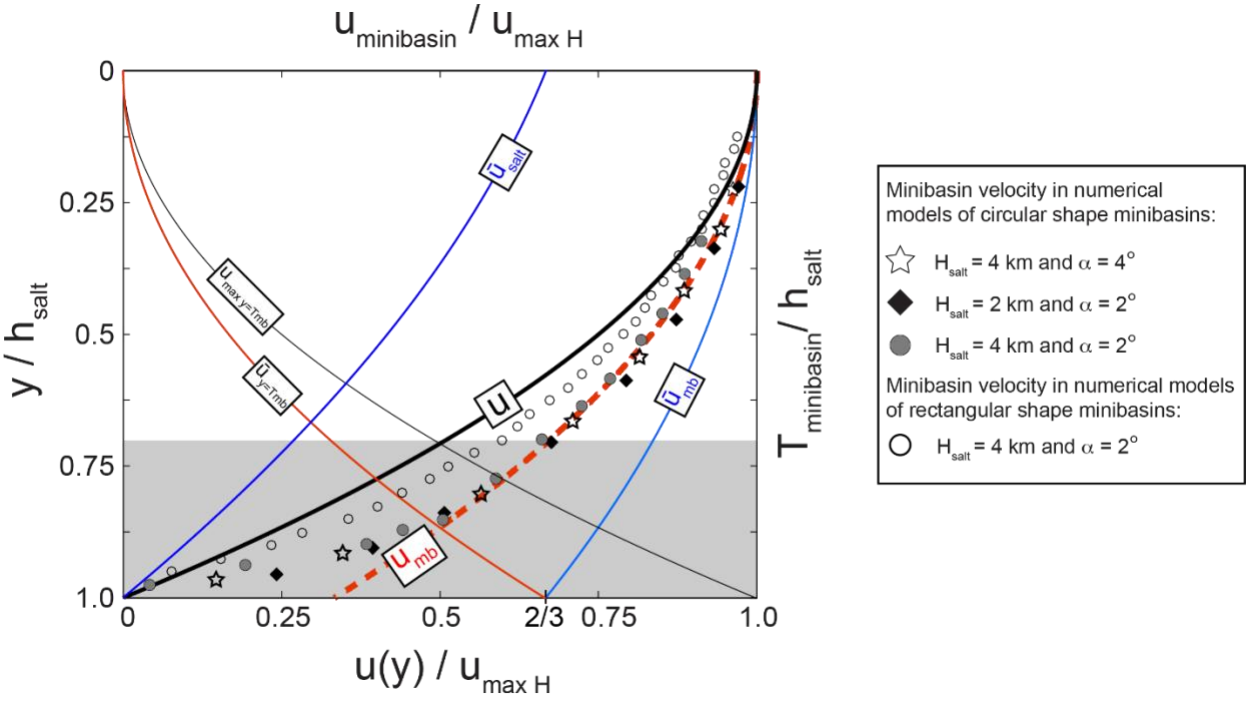

Figure SI-A4. Normalized plot with the solid-line graphs corresponding to the 1D channel flow derived equations as described in the text. Markers correspond to results of 2D numerical simulations with rectangular minibasins (hollow circles) and circular minibasins (grey circles, black diamonds, hollow starts) for the simulation parameters shown in the legend.

The numerical models show that thin minibasins translate faster than thick minibasins. The relation between thickness and minibasin velocity in the case of minibasins of circular shape describes a curve in the graph. In fact, the results from the numerical simulations with minibasins plot on top of a curve that can be described by the following equation,

$$u_{mb} = u_{\max\ h} - \bar{u}_{y=Tmb} = \frac{\bar{u}_{mb}+u(y)}{2} = \frac{\rho\ g\ sin\alpha\ h^2}{\mu\ 2} - \frac{\rho\ g\ sin\alpha\ y^2}{\mu\ 3} \quad \text{(A31) or } \mathbf{Eq.\ (4)}$$

Eq. (4) is used in the main text to predict the velocity of sub-circular minibasins in the numerical simulations.

However, the minibasins with a rectangular shape (vertical walls), plot closer to the graph described by $u(y)$. In addition, Increasing the length (width) of the minibasin, but keeping their thickness the same, reduces minibasin velocity, moving the velocity value in the graph to the left. The lower limit for the velocity of a minibasin of given thickness is the velocity described by u(y). The velocities calculated in numerical simulations with minibasins of different geometries (aspect ratios, sub-circular or rectangular), plot in the area of the graph between $u(y)$ and u_{mb}.

Thus, although the equations are derived for 1D channel flows, they can be used to predict the velocity of sub-circular minibasins as shown in the main text.

References

Turcotte, D.L. and Schubert, G., 2002. Geodynamics. Cambridge University Press. New York. 456 p.

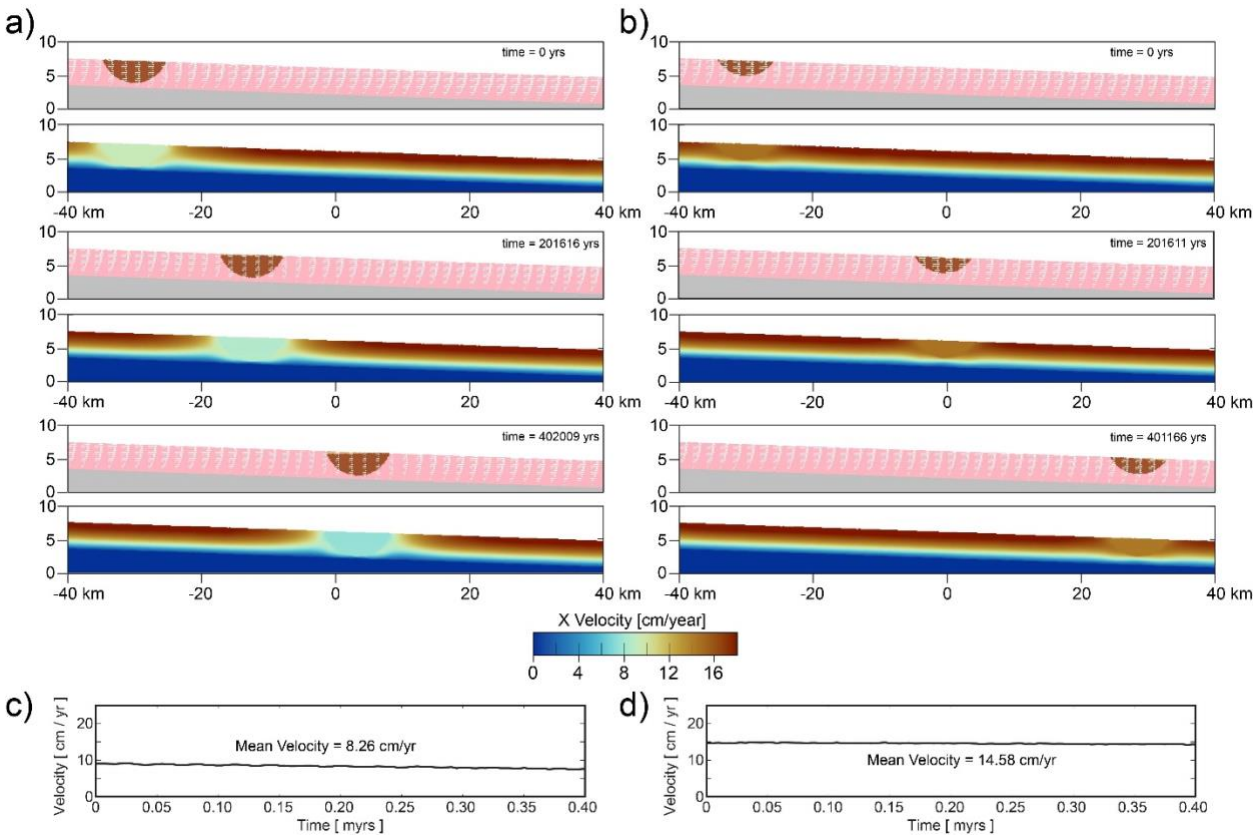

Figure SI-5. a) and b) Screenshots with plots of composition and velocity field of three different time steps of two numerical simulations of salt moving downslope. a) Simulation with thick minibasin b) Simulation with thin minibasin. c) and d) Graphs with the evolution through time of the mean velocity of the minibasin from the two simulations. c) Simulation with thick minibasin. d) Simulation with thin minibasin. Note that the thin minibasin has higher velocity through time (c) and thus, higher mean velocity than the thick minibasin (d). The higher velocity of the thin minibasin results in the thin minibasin having advanced further than the thick minibasin in the screenshots shown in (a) and (b).

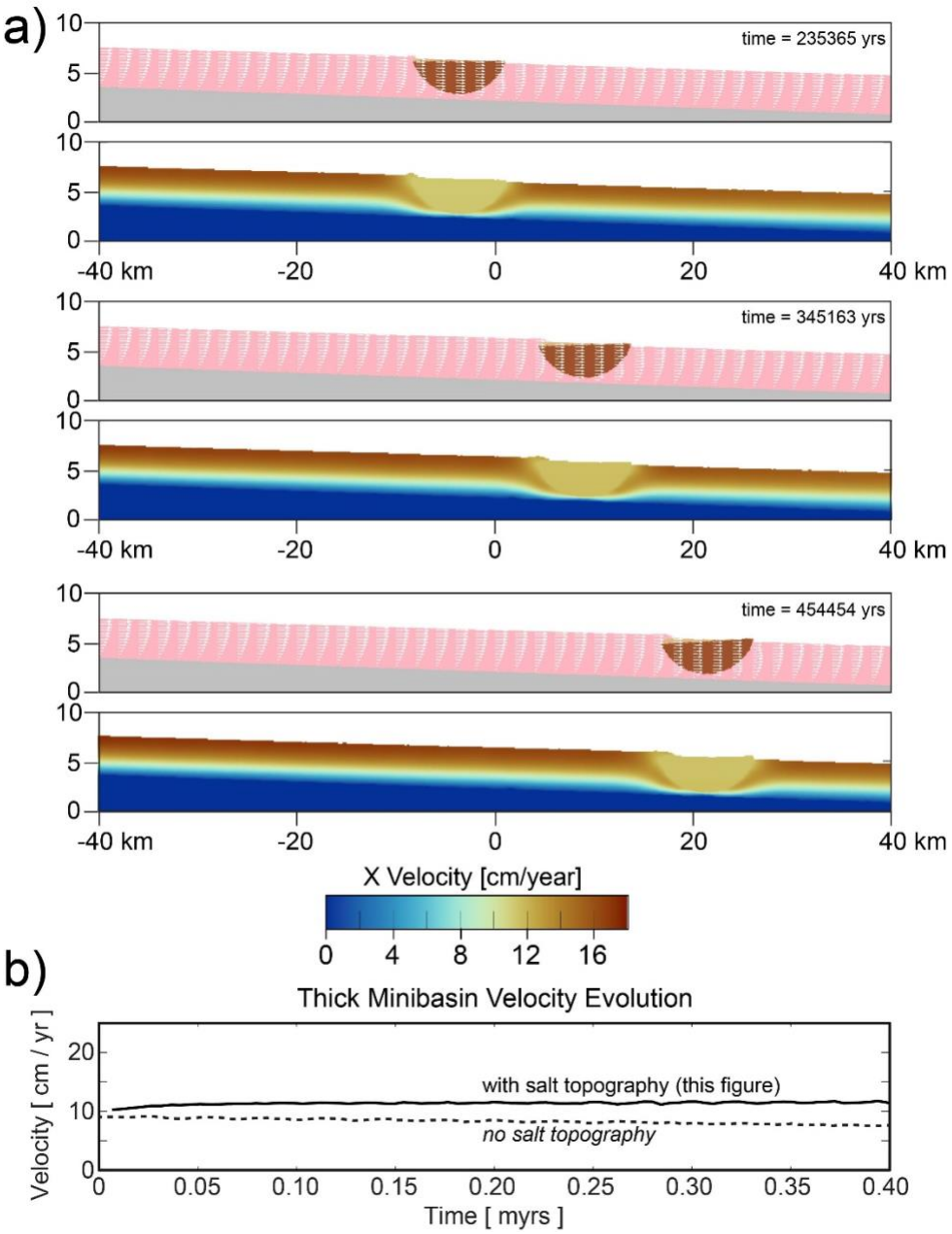

Figure SI-6. a) Screenshots of four time-step evolution of a numerical simulation with a thick minibasin. In this simulation, implemented boundary conditions, allowed for the development of salt topography. As a result, shallow, faster moving salt is extruded on top of the slow moving minibasin during the translation. b) Graph showing the velocity evolution of the minibasin in the simulation with salt topography (continuous black line, simulation shown in this Figure), and of the minibasin in the simulation with no-salt topography allowed (dashed black line, simulation shown in previous Figure). Note that in the simulation where salt-topography could develop the minibasin velocity increased with time. In this particular case where, the average velocity of the thick minibasin is dramatically slower than velocity of the shallow (i.e. upper) portion of the salt, and the faster-flowing salt up-dip of the minibasin extrudes onto the minibasin. The load of the salt extrusion on top of the minibasin enhances the tilt of the minibasin and the overall effect of the process is a slight increase of the minibasin velocity through time.

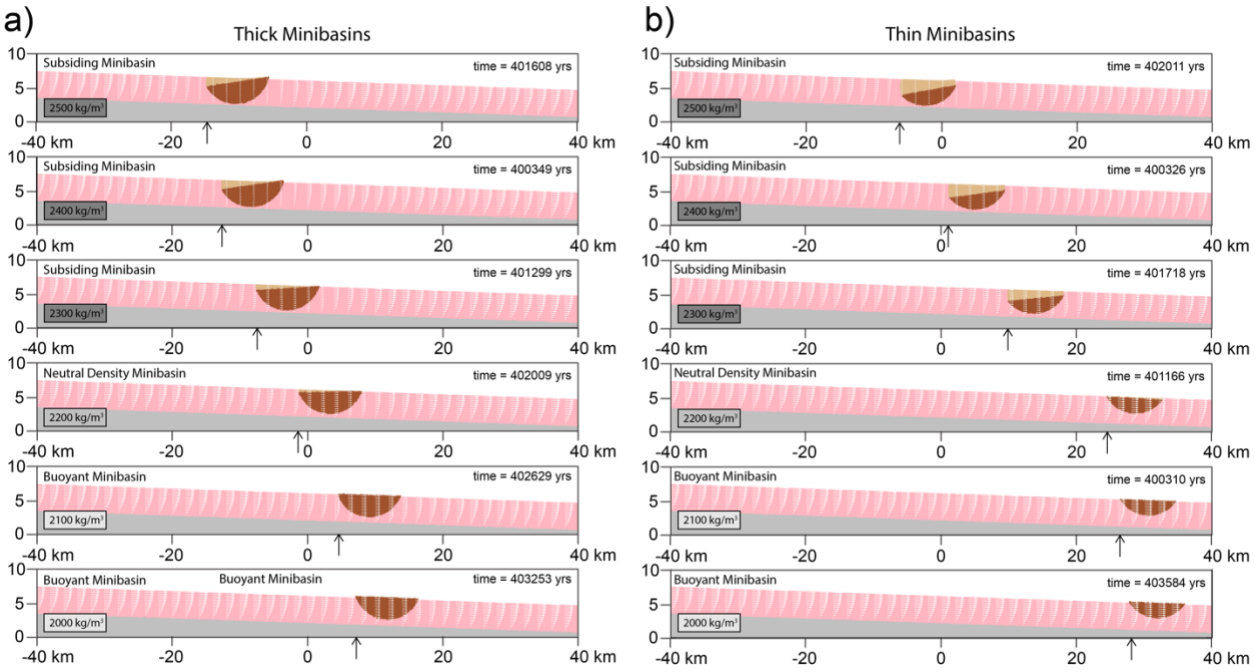

Figure SI-7. a) and b) Screenshots at the same final time step (time =~400000 yrs.) of numerical simulations with thick (a) and thin (b) minibasins of different densities. The amount of minibasin translation varies according to their densities. Upper panels show the highest density minibasins (denser than salt) and have the least amount of translation (a, b). For simulations with different minibasin densities, final minibasin translation is higher (a, b). Highest minibasin translation is seen at the lower panel (lowest density minibasin, less dense than salt). Minibasins that are denser than salt subside as they translate downslope, allowing for sediment accumulation in their up-slope edge. The accumulation of new sediment results in an increase of minibasin thickness trough time.

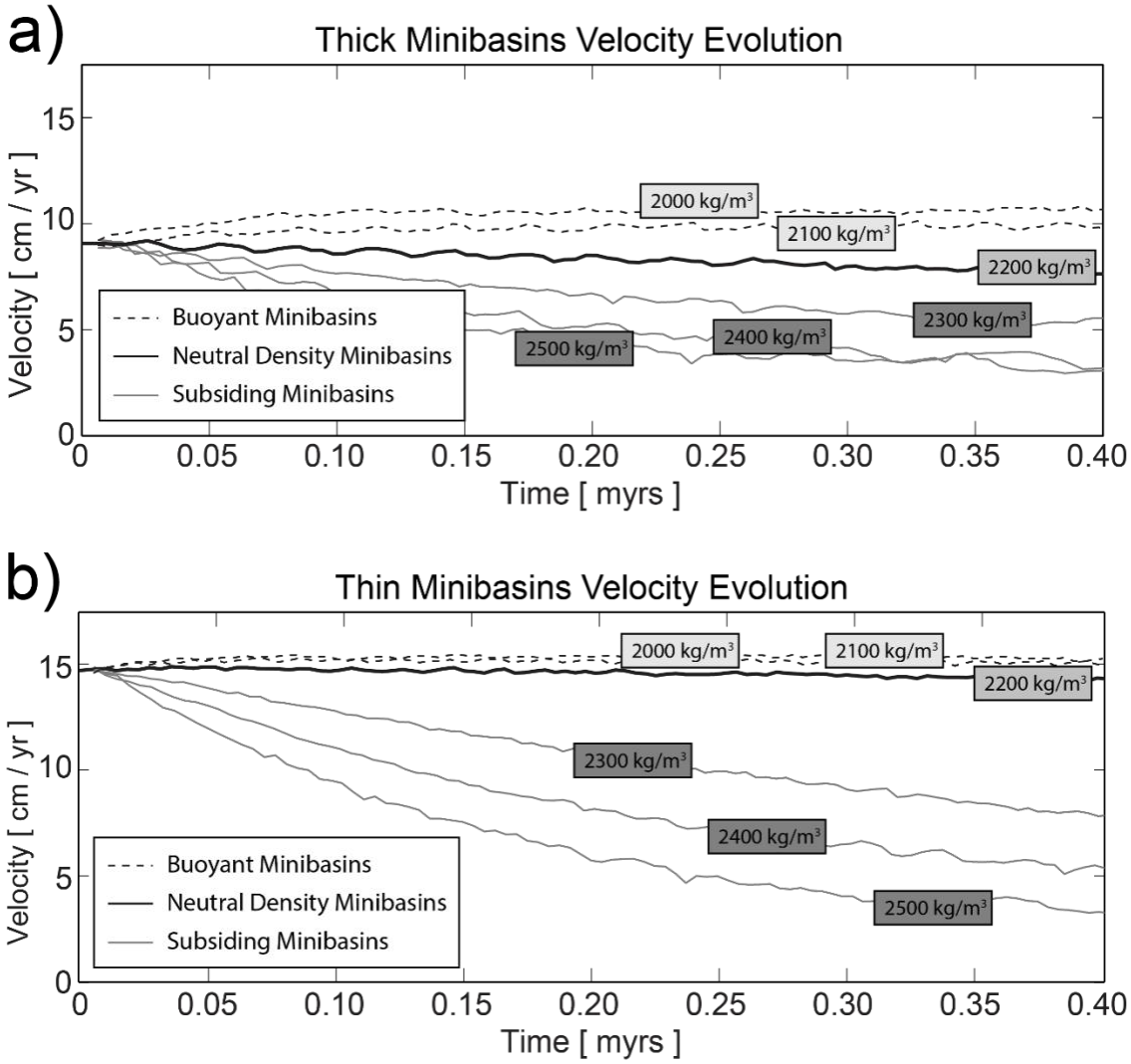

Figure SI-8. Graphs showing the velocity evolution in simulations with minibasins whose density is different than that of the salt. a) Simulations with thick minibasins. b) Simulations with thin minibasins. Note that, when minibasins are denser than the salt, the velocity of the minibasins tend to decrease through time. Also, the higher the density the faster the decrease in the velocity it is. The opposite is true for minibasins that are less dense than salt, which increase their velocity through time.

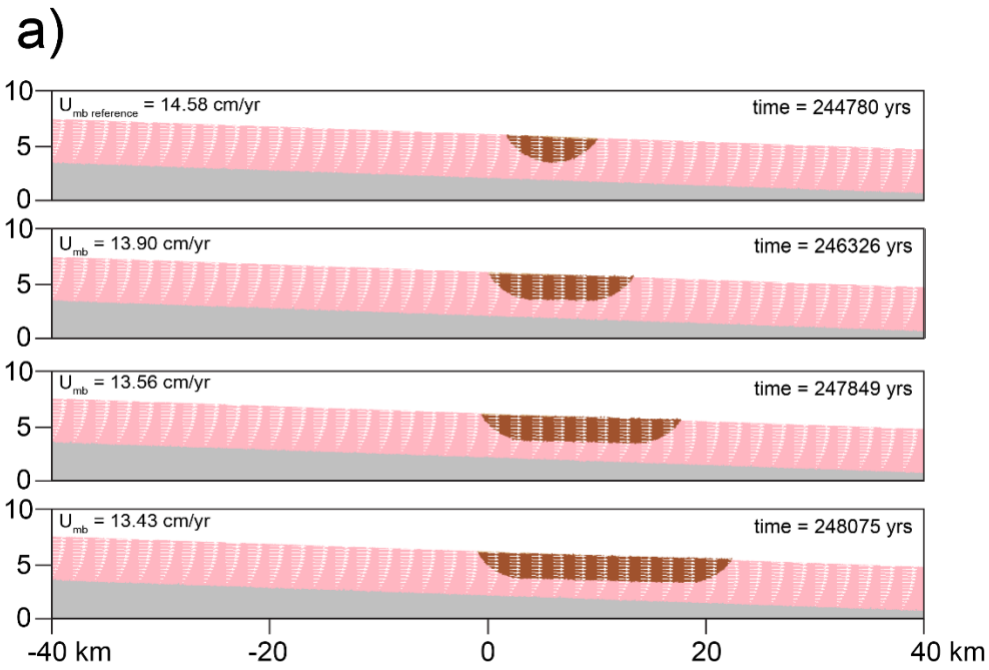

Figure SI-9. a) Screenshots at the same time-step of four simulations with neutral-density minibasins of same initial thickness but different length or aspect ratio. The minibasin to salt thickness of this example is T_{mb}/H_{salt} = 0.575. The arrow indicates the center of the minibasin, which at the beginning of the simulations was located at the same position for all for cases. The arrow at this time step illustrates, that although there has been differential translation, the amount is relatively small. The longest minibasin, which has the highest aspect ratio, (lower panel) has the slowest mean velocity of all, although the differences are relatively small.

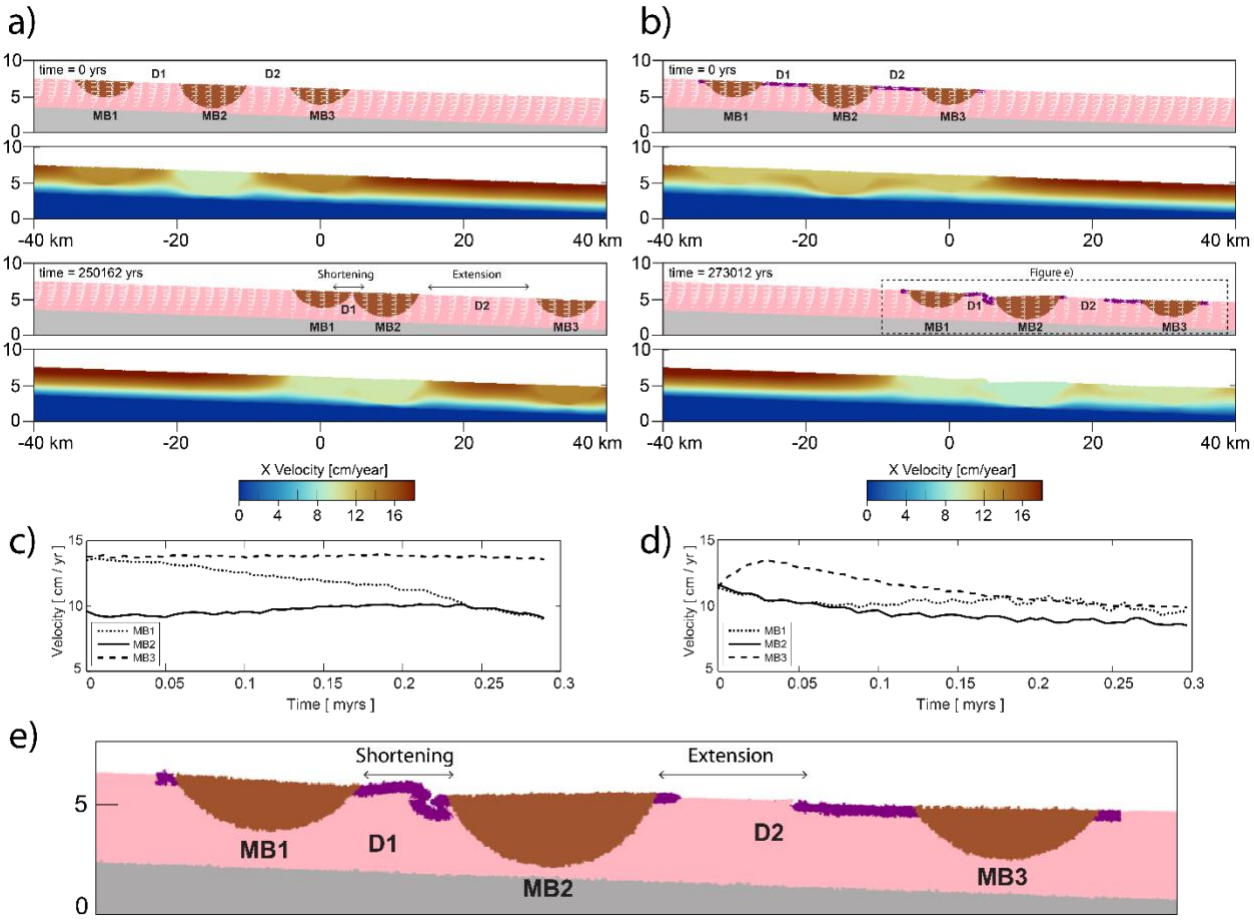

Figure SI-10. Screenshots of a three time-step evolution of a chain of three neutral-density minibasins on a slope (from updip to downdip, MB1, MB2 and M3; with intervening diapirs D1 and D2). The minibasin in the center (MB2) is thicker than the ones updip and downdip. Two scenarios are shown. One scenario in which the diapirs are exposed and not covered by a roof (a), and one in which the diapirs are covered by a roof on top (b). The velocities of the minibasins for each scenario are plotted in c) and d). In the simulation with the exposed diapirs (a), as the numerical simulation evolves, the thin minibasins (MB1 and MB3) translate faster than the thick minibasin (MB2) (c). However, as the simulation evolves, updip thin minibasin (MB1), decreases its velocity as it approaches the thick minibasin MB2 (c). In the simulation with covered diapirs (b), because the three minibasins are initially connected by the roof, their starting velocities are the same (d). However, as the simulation evolves, the downdip minibasin (MB3) drifts away from the minibasin in the center (MB2), the roof in between the two gets stretched (b, d). Instead, the minibasin updip (MB1), converges towards the minibasin in the center and the roof in between gets shortened by folding (b, c). e) Zoomed view of the rectangle of Figure b) where the deformation of the roof above the diapirs can be observed.

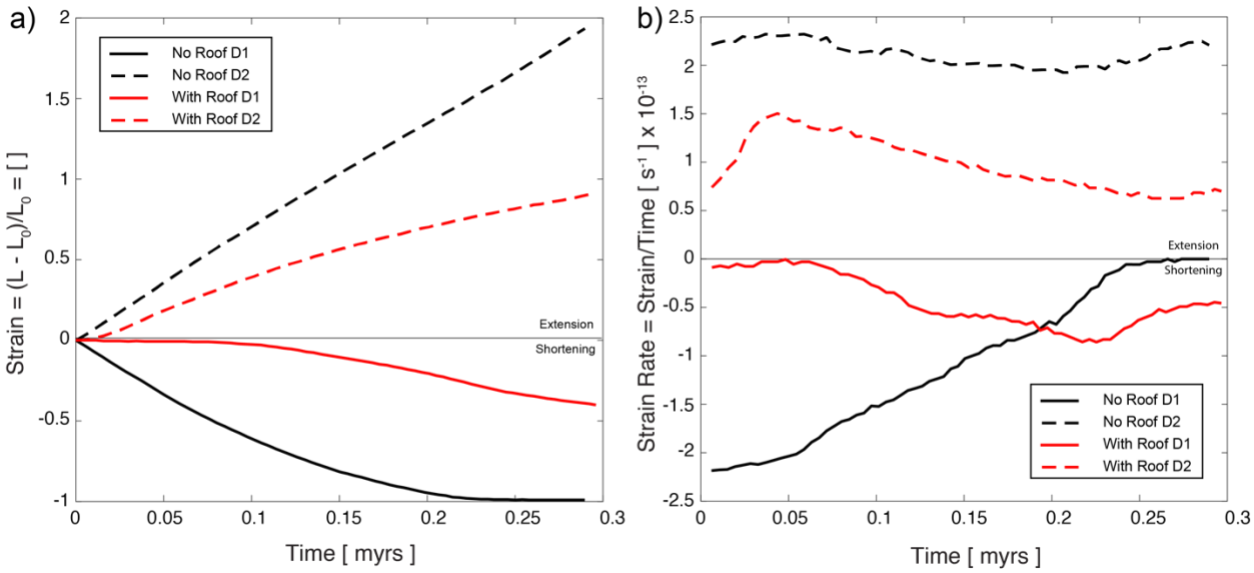

Figure SI-11. a) Strain accommodated by the diapirs D1 and D2, for the simulations with no roof and without roof. D1 is the diapir located upslope, in between the converging minibasins MB1 and MB2. As such, diapir D1 accommodates the shortening, as shown by negative value of the strain. The opposite is true for diapir D2, which is located downslope, between diverging minibasins MB2 and MB3. It must also be noted, the higher amount of strain, whether extensional or compressional, accommodated by the case in which the diapir has no roof. b) Strain rate calculated for the diapirs D1 and D2. The negative value of the strain rate indicates the shortening which is being accommodated by diapir D1. Notice, how in the case of the diapir with roof, the strain rate remains close to zero initially, meaning that there is no strain being accommodated by the roof. This is very different to what it is observed in the case with roof. Additionally, in the case of the diapir D2, both the cases with roof and no-roof start accommodating the deformation early in their evolution.